Inorganica Chimica Acta, *193* (1992) 57–75

Polynuclear transition metal complexes. The reactivity of the new potentially binucleating ligand 2,6-diacetylpyridine-bis(1′-phthalazinylhydrazone) towards Ni^{II}, Cu^{II} and Zn^{II} salts, and crystal and molecular structure of {bis[2,6-diacetylpyridine-bis(1′-phthalazinylhydrazonato)nickel(II)]} dimethylformamide and water solvate

G. Paolucci*, S. Stelluto

Dipartimento di Chimica, Università di Venezia, Calle Larga S. Marta 2137, 30123 Venice (Italy)

S. Sitran, D. Ajò, F. Benetollo, A. Polo

Istituto di Chimica e Tecnologia dei Radioelementi, Area di Ricerca C.N.R., Corso Stati Uniti, 4, 35100 Padua (Italy)

and G. Bombieri

Istituto di Chimica Farmaceutica, Università di Milano, Milan (Italy)

(Received June 27, 1991; revised October 31, 1991)

Abstract

The interaction of the new, potentially binucleating, ligand 2,6-diacetylpyridine-bis(1′-phthalazinylhydrazone) (H_2dapz), containing only nitrogen donor atoms, towards nickel(II), copper(II) and zinc(II) salts is reported. Depending on the nature of the counteranions, Ni^{II} and Cu^{II} ions selectively enter in one of the two 'compartments' present in the ligand. Analytical and spectroscopic characterizations of five series of mononuclear complexes [dapzM], [H_2dapzMCl_2], [HdapzMCl], [(H_2dapz)$_2$M][ClO_4]$_2$, [HdapzM][ClO_4], coming from reactions of metal acetates, metal chlorides and metal perchlorates, respectively, and the ligand in the bisdeprotonated, monodeprotonated and undeprotonated forms, are reported together with some interconversion reactions. Some tentative stereochemical assignments of these compounds are reported on the basis of their physicochemical properties. Different behaviour has been observed in the case of zinc(II) chloride and perchlorate. Crystal structure analysis on the bisdeprotonated complex [dapzNi]$_2$, shows that the compound is dimeric, with the metal ions octahedrally coordinated into the upper compartment, and the pyridine nitrogens bridging the two nickel atoms.

Introduction

During the last decade, a number of binucleating ligands have been synthesized with the aim of studying the peculiar properties of their corresponding binuclear complexes in different fields, i.e.

(i) in homogeneous catalysis, as species capable of carrying out multistep reactions of different successive processes [1];

(ii) in biochemistry as potential models for the study of biological reactions involving molecular oxygen, such as oxygen transport [2] and oxygen activation [3–5], reproducing the enzymatic natural systems [6];

(iii) for magnetochemical studies, mainly in exchange interactions of heterobinuclear complexes [6–11].

In recent years binucleating ligands containing only nitrogen as ligating atoms have received particular attention and have been based largely on substituted 'diazine' type units. Polyfunctional ligands derived from hydrazine [12–14], pyrazole [15–19], pyridazine [5, 20–26] and phthalazine [15, 20, 22–40], form binuclear transition metal complexes where the metal ions are brought into close proximity because of the geometric requirements of the =N–N=, diazine, fragments in these systems. Phthalazine and pyridazine systems have been shown by a number of researchers to provide the binucleating centre for many Co^{I}, Co^{II}, Ni^{II}, Cu^{II} and Zn^{II} complexes [22–40], where the interaction between the two metal ions is transmitted through the π-electron system of the diazine group, thus affecting both the magnetic behaviour and the reactivity of the mononuclear species.

---

*Author to whom correspondence should be addressed.

0020-1693/92/$5.00

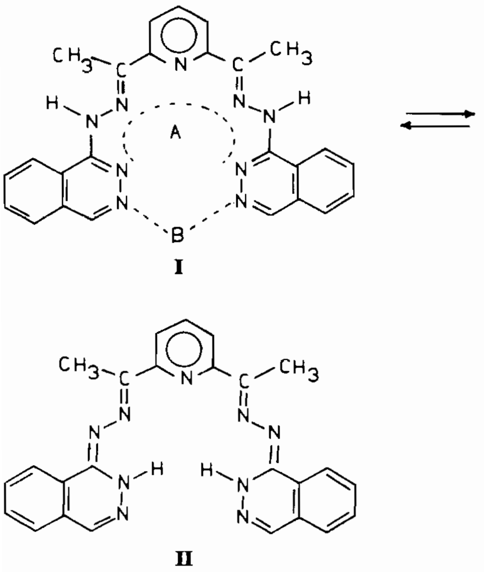
I

II

Fig. 1. The tautomeric forms of the ligand H_2dapz.

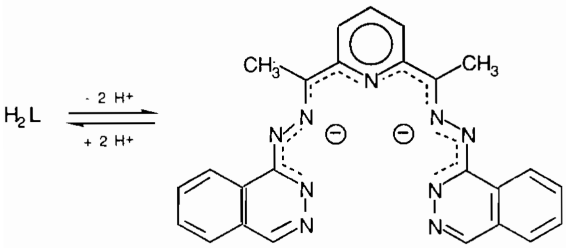

Fig. 2. The resonance forms of the bisdeprotonated ligand $dapz^{2-}$.

1,4-Dihydrazinophthalazine is a reactive intermediate, which acts as a tetradentate binucleating ligand in its own right [22, 24, 29], and reacts with appropriate aldehydes or ketones to form the corresponding hydrazones [27, 32, 38, 39]. Owing to the presence of identical coordination sites, these ligands only afford homobinuclear complexes.

Looking at the heterobinucleating systems, we synthesized the new ligand 2,6-diacetylpyridine-bis(1′-phthalazinylhydrazone) (H_2dapz, dapz = L) containing in principle, two different coordination compartments (Fig. 1):

(i) a potentially tri-, tetra- or pentadentate site (A); and

(ii) a bidentate site (B).

Due to the different extent of the chelating effects the two compartments could, in principle, prevent any formation of homobinuclear species by reacting with transition metal salts in a 1:1 molar ratio. In fact, the coordination of the metal ion into compartment A could preferentially give rise to the formation of five-membered chelating rings with respect to the coordination into compartment B. The presence in this ligand of two deprotonable hydrazonic hydrogens makes it possible to obtain several classes of complexes containing the ligand in the various deprotonated forms (H_2dapz, $Hdapz^-$ and $dapz^{2-}$) (Fig. 2).

Experimental

Materials

Reagent grade 2,6-diacetylpyridine, 1-hydrazinophthalazine hydrochloride (Hydralazine) were purchased from Janssen Chimica (Beerse, Belgium), and used without further purification. Proton Sponge (*N*,*N*,*N*′,*N*′-tetramethyl-1,8-naphthalenediamine) (Janssen product) was recrystallized from benzene and maintained under an inert atmosphere in a dry box. All inorganic hydrate salts were purchased from Alpha Inorganics and used without further purification.

Instrumentation

^1H NMR spectra of the ligand and the diamagnetic zinc(II) complexes were obtained in deuteriochloroform or DMSO-d_6 solutions on a Varian Associates FT-80A spectrometer. IR spectra (4000–200 cm^{-1}) were obtained (KBr disks or Nujol mulls on CsI plates) on a Perkin-Elmer 683 spectrometer. Electronic spectra (chloroform or dimethylformamide solutions) were recorded on a Cary 17D spectrophotometer.

Elemental analyses of the complexes were performed by Professor E. Celon of the Department of Organic Chemistry of the University of Padua. Analyses of the metal ions were performed using either an A. A. Perkin-Elmer 2380 or complexometric techniques.

X-ray measurements and structure determination

The crystal and refinement data for $Ni_2L_2 \cdot [(CH_3)_2NCHO] \cdot H_2O \cdot 0.5CH_3CH_2OH$ (red–brown transparent regular prisms) are summarized in Table 1. A prismatic single crystal of dimensions $0.25 \times 0.09 \times 0.11$ mm was centered on a four-circle Philips PW1100 diffractometer equipped with graphite monochromated Mo Kα radiation. The orientation matrix and preliminary unit cell dimensions were determined from 25 reflections found after mounting the crystal at random and varying each of the orientation angles χ and Φ over a range of 120°, with the detector position barying between $12 \leq 2\theta \leq 20°$. For the determination of precise lattice parameters 25 strong reflections with $9° \leq \theta \leq 14°$ were considered.

The intensities of the two standard reflections, 5 2 2 and 4 0 2, were monitored every 180 min. No significant fluctuation in intensities other than those expected from Poisson statistics were observed.

TABLE 1. Crystallographic data for $Ni_2O_{2.5}N_{19}C_{54}H_{50}$

Chemical formula	$Ni_2O_{2.5}N_{19}C_{54}H_{50}$
Formula weight	1122.5
Space group	$P2_1/a$ (No. 14)
a (Å)	21.573(3)
b (Å)	22.118(3)
c (Å)	10.892(2)
β (°)	93.66(4)
V (Å^3)	5187(1)
Z	4
T (°C)	22
λ (Å)	0.71069
ρ_{obs}	(g cm^{-3}) 1.43
ρ_{calc}	(g cm^{-3}) 1.44
μ	(cm^{-1}) 7.36
Transmission coefficient (rel.)	85/100
$R = R(F_o)$	0.052
$R_w = R_w(F_o)$	0.051
GOF	1.43

The intensities were corrected for Lorentz–polarization effects and for absorption, following the method of North *et al.* [41]; no correction was made for extinction.

The structure was solved using direct methods and Fourier techniques and refined by full matrix least-squares, with anisotropic thermal parameters for Ni and for the ligating atoms and isotropic thermal parameters for the remaining non-hydrogen atoms. Hydrogen atoms were introduced in calculated positions (d(C–H) = 0.95 Å and U_{iso} = 0.07 Å). The refinement of the $[Ni(dapz)]_2[(CH_3)_2NCHO]\cdot H_2O$ complex reached convergency at R = 0.063. At this point three residuals of about 2 e/Å^3 were evident in the Fourier difference map. They were interpreted as a statistically distributed half molecule of ethanol per $[Ni(dapz)]_2[(CH_3)_2NCHO]\cdot H_2O$ unit. The introduction of the ethanol molecule in the positions indicated by the electron density residuals with population factors of 0.5 gave the most significant lowering of the R values R = 0.052 and R_w = 0.051. The anomalous dispersion terms for Ni were taken into account in the refinement. Atomic scattering factors were taken from ref. 42. Data processing and computation were carried out by using the SHELX 76 program package [43], and PLUTO [44] for drawing.

Magnetic measurements

Magnetic susceptibility values were measured by the Faraday method over the 67–295 K range, the apparatus (Oxford Instruments, equipped with a CF200 cryostat and a Cahn 2000 microbalance) being calibrated with $HgCo(NCS)_4$ [45]. Diamagnetic corrections were carried out [46]. χ was measured at different fields in the range 1–1.2 T (10 000–12 000 gauss). In this range χ (hence μ) does not significantly depend on field.

Preparation of the ligand 2,6-diacetylpyridine-bis(1′-phthalazinylhydrazone) (H_2dapz)

To a solution of 1-hydrazinophthalazine hydrochloride (1.96 g, 10 mmol) in a mixture of absolute ethanol:pyridine (75:25, vol.:vol.) (200 ml), an ethanolic solution (50 ml) of 2,6-diacetylpyridine (0.816 g, 5 mmol) was added at 80 °C, and the mixture refluxed for 3 h. The yellow precipitated product was filtered, washed several times with hot ethanol (20 ml portions) and dried *in vacuo* (2.180 g, 97.5% yield). *Anal.* Calc. for $C_{25}H_{21}N_9$: C, 67.11; H, 4.70; N, 28.19. Found: C, 67.37; H, 4.34; N, 27.76%.

*Synthesis of bisdeprotonated complexes **Ia–c** (**a** = Cu, **b** = Ni, **c** = Zn) (general procedure)*

To a suspension of the ligand H_2L (0.447 g, 1 mmol) in pyridine (30 ml), an ethanolic solution (40 ml) of metal acetate hydrate (1 mmol) was added, and the resulting mixture stirred at 50 °C for 3–4 h. The solid products were filtered, washed several times with absolute ethanol portions and dried *in vacuo* (90–95% yields), giving microcrystalline, analytically pure products. Recrystallization of **Ib** from DMF: diethyl ether affords dark brown crystals suitable for X-ray analysis.

*Synthesis of adducts **IIa–c** (general procedure)*

To the ligand H_2L (0.447 g, 1 mmol) suspended in absolute ethanol (50 ml), an ethanolic solution (20 ml) of the metal chloride hydrate (1 mmol) was dropwise added at 50 °C and the resulting mixture stirred for 3–5 h at the same temperature. The precipitated products were filtered, washed several times with absolute ethanol (5 ml portions; slight solubility) and dried *in vacuo*. The yields were in the range 90–95%. **IIa** was crystallized from methanol giving brown needles. **IIc** was crystallized from dichloromethane:benzene (3:1; vol.:vol.) giving yellow–orange needles suitable for X-ray analysis.

Normally **IIb** is formed together with variable amounts (5–10%) of **IIIb**. By crystallization from DMF:diethyl ether red–brown crystals of **IIe** were obtained.

When using the ligand with copper(II) and zinc(II) chlorides the use of larger volumes of alcohols (either ethanol or methanol) did not affect the formation of the adducts **IIa** and **IIc** respectively. In contrast, by carrying out the reaction of the ligand and $NiCl_2\cdot 6H_2O$ in the same molar ratio 1:1, but in a 10 times larger volume of ethanol than previously reported, either at room temperature or at 50 °C, the only product isolated, after concentration, was the monodeprotonated species **IIIb**. The same results were obtained by using anhydrous $NiCl_2$ and anhydrous absolute ethanol (500 ml) in inert atmosphere (argon).

Synthesis of IId and IIe

To a solution of the ligand (0.447 g, 1 mmol) in DMF (or DMSO) (80 ml) a solution of $NiCl_2 \cdot 6H_2O$ (0.237 g, 1 mmol) in absolute ethanol (20 ml) was added at 80 °C and the mixture was stirred for 3 h. The microcrystalline red–brown **IIe** (or dark brown **IId**) that precipitated during the reaction, was filtered, washed several times with ethanol portions and dried at 80 °C *in vacuo* (87% yield). The same products were obtained by crystallization of crude **IIb** from DMF:EtOH or DMSO:EtOH.

Synthesis of IIIa and IIIb

The monodeprotonated species **IIIa** and **IIIb** were prepared according to the following methods:

(a) From H_2dapz and metal chlorides in ethanol/pyridine mixtures as solvent

To the ligand (0.447 g, 1 mmol) suspended in ethanol/pyridine (2:1; vol.:vol.) (60 ml), a solution of the metal chloride hydrate (1 mmol) in ethanol (10 ml) was added at 50 °C. The resulting mixture was refluxed for 3–4 h. The dark coloured solids were filtered, washed several times with absolute ethanol (5 ml portions) and dried *in vacuo* (80% yield).

(b) By monodeprotonation of IIa and IIb with Proton Sponge

To a solution of **IIa** or **IIb** (1 mmol) in absolute ethanol (250 ml), Proton Sponge (1 mmol) dissolved in absolute ethanol (10 ml) was added at room temperature. The reaction mixture was left to react under magnetic stirring at room temperature for 48 h. The solvent was evaporated under reduced pressure up to 60 ml. After cooling the precipitated solids were collected by filtration, washed with ethanol and dried *in vacuo* (70–80% yield). The same monodeprotonated species were obtained by crystallization of the adducts **IIa** and **IIb** from absolute ethanol:water (99:1; vol.:vol.).

(c) By monoprotonation of Ib with HCl

To a solution of **Ib** (1 mmol) dissolved in absolute ethanol (250 ml), a solution of conc. HCl (0.168 ml, 2 mmol) in absolute ethanol (20 ml) was added at room temperature. The colour of the solution changed from dark brown to red–brown and a brown product started to precipitate. The mixture was stirred at room temperature for 3 h (by increasing the reaction time no change in the product was observed). The solid product was filtered, washed with absolute ethanol and dried *in vacuo* (80% yield).

In the same conditions **Ia** afforded a hardly separable mixture of products (**IIa** and **IIIa**).

The adduct **IIc** never afforded the monodeprotonated species following the procedures (a), (b) and (c). In all cases the ligand was recovered as main product.

Reaction of IIIa and IIIb towards Proton Sponge (1:1)

To a suspension of the monodeprotonated species (**IIIa** or **IIIb**) (0.5 mmol) in absolute ethanol (80 ml) a solution of Proton Sponge (0.5 mmol) in the same solvent (20 ml) was added at room temperature. The mixture was stirred for 3 h, and the precipitated products were collected by filtration, and identified by their physicochemical properties as the bisdeprotonated species (**Ia** or **Ib**).

Reaction of IIa and IIb towards Proton Sponge (1:2)

To the adducts **IIa** or **IIb** (0.5 mmol) suspended in dichloromethane (100 ml), a solution of Proton Sponge (1 mmol) in the same solvent (10 ml) was added at room temperature. The mixture was stirred until complete solubilization was achieved (40 h). By concentration of the solution under vacuum **Ia** or **Ib** precipitated. The filtered products were washed sequentially with H_2O, EtOH and Et_2O, and dried *in vacuo.*

Reaction of IIc towards Proton Sponge

By addition of Proton Sponge to a solution of **IIc** (0.5 mmol) in dichloromethane (100 ml) in molar ratio 2:1, at room temperature, the ligand H_2L was quantitatively obtained. The same behaviour was observed by crystallization of IIc from pyridine:absolute ethanol (2:1, vol.:vol.).

By reacting at room temperature IIc and Proton Sponge in dichloromethane, in molar ratio 1:1, the ligand H_2L precipitated (48% yield). After the ligand was filtered off, the addition of n-hexane to the filtrate caused the precipitation of **IIc** (46% yield).

Synthesis of IVa and IVb (general procedure)

To a suspension of the ligand (0.894 g, 2 mmol) in absolute ethanol (80 ml), a solution of metal perchlorate hydrate (1 mmol) in the same solvent (20 ml) was added at 80 °C. The mixture was refluxed for 10 h. After cooling, the precipitated products were filtered, washed several times with absolute ethanol and dried *in vacuo* (85–90% yields). The crude products were analytically pure. Crystallizations were made from absolute ethanol. In DMF, DMSO and acetonitrile, both **IVa** and **IVb** liberated the ligand H_2L.

Synthesis of $[HLCu \cdot 2H_2O][ClO_4]$ (Va) and $[HLNi][ClO_4]$ (Vb)

To the ligand (0.447 g, 1 mmol) suspended in hot absolute ethanol (40 ml), a solution of the hydrated metal perchlorate (1 mmol) in the same solvent (10 ml) was added dropwise. The reaction mixture was reacted at reflux for 12 h. Then, the precipitated product formed (**Va** or **Vb**) was filtered, washed with absolute ethanol and dried *in vacuo* (75–82% yield). Successful crystallizations were made from ethanol. The same products **Va** and **Vb** were obtained by reaction at room temperature of **Ia** and **Ib**, respectively, with $HClO_4$ in molar ratio 1:2, in absolute ethanol.

Results and discussion

Scheme 1 summarizes the reactions of the ligand H_2dapz toward Ni^{II}, Cu^{II} and Zn^{II} salts, and the interconversion reactions that the various complexes undergo. In order to make the discussion more easy the various species **I**, **II**, **III**, **IV** and **V**, will be discussed separately.

Bisdeprotonated species [dapzM]$_x$ (I)

All the three metal acetates react with the ligand in molar ratio 1:1 to afford, in high yields, the bisdeprotonated mononuclear complexes **Ia**, **Ib** and **Ic**, free of any homobinuclear species. Probably these nonconducting (in $CHCl_3$, MeOH and CH_3CN solutions) species are obtained from preliminary formed adducts (formed in compartment A), where the increased acidity, by coordination with the metal ion, of the hydrazonic protons makes possible the deprotonation by the acetate ion to species **I**. As a confirmation, the deprotonation takes place in EtOH/pyridine as well as in pure EtOH.

Tables 2 and 3 summarize the analytical and physicochemical data of the **Ia**, **Ib** and **Ic** complexes.

The IR spectra of **Ia**, **Ib** and **Ic** complexes are very similar to one another (**Ia** and **Ic** are almost identical) and are characterized by the lack of the N–H stretching band, present in the free ligand (3340 cm^{-1}) and by the appearance of a medium-weak band at 1580 cm^{-1} (in the free ligand two bands at 1610 and 1595 cm^{-1} are due to pyridine and phthalazine vibrations) and a very strong band at 1500 cm^{-1} characteristic of the coordinated C=N–N=C system [47], together with some other shifted bands due to the coordinated heterocyclic systems.

As a confirmation of this hypothesis, the IR spectra of the species **Ia**, **Ib** and **Ic** show medium-weak bands at 1015 cm^{-1} due to coordinated pyridine (in the free ligand the same band is at 998 cm^{-1}) [33]. To date no assignments of ν(M–N) relative to the pyridine nitrogen bridging two metal ions have been reported, thus the assignement of this band is quite difficult, due to the presence of a number of weak bands in the range 400–250 cm^{-1}, typical of ν(M–N) of phthalazine and pyridine rings [35].

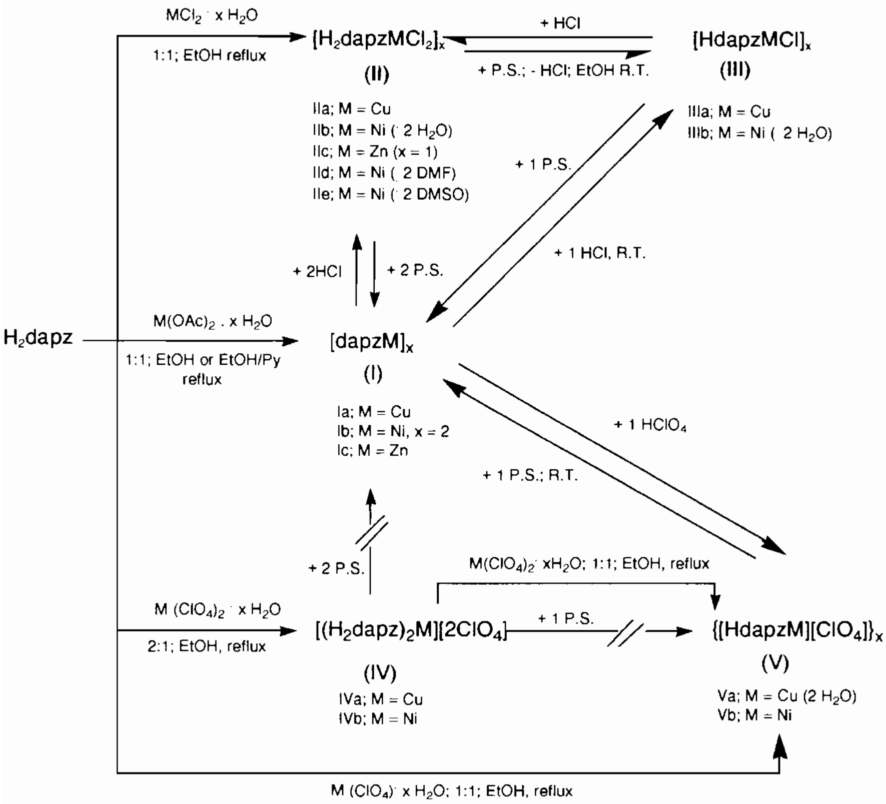

Scheme 1.

TABLE 2. Analytical and physicochemical data of species I

Complex	Color (yield (%))	Elemental analysis					μ^a	Electronic spectra^b	
			C	H	N	M		(cm^{-1})	ϵ
$\{[LCu]\}_2$ (**Ia**)	bronze (89)	Found	58.50	3.80	24.20	12.60	1.90	34965 33134 22124	27146 33131 14037
		Calc. for $C_{50}H_{38}N_{18}Cu_2$	58.98	3.76	24.78	12.49		13889	294
$\{[LNi]\}_2$ (**Ib**)	dark brown (92)	Found	59.05	3.70	24.80	11.75	2.84	35714 22091 21739	30843 36973 25060
		Calc. for $C_{50}H_{38}N_{18}Ni_2$	59.53	3.80	25.01	11.65		18657 13889	7325 347
$\{[LZn]\}_2$ (**Ic**)	orange	Found	58.60	3.90	24.20	12.95		35335 33134	22253 35586
		Calc. for $C_{50}H_{38}N_{18}Zn_2$	58.76	3.71	24.69	12.80		21739	11712

[a] At room temperature. [b] In chloroform solution.

TABLE 3. Main IR bands characteristic of species I (cm^{-1})

Complex	C=C, C=N^a (pyridine and phthalazine)	ν(M–N)^b	Pyridine ring breathing
[LCu] (**Ia**)	1590	348	1015
	1550	310	
	1530	290	
	1495	270	
[LNi] (**Ib**)	1590	348	1015
	1535	318	
	1490	270	
[LZn] (**Ic**)	1590	378	1015
	1550	352	
	1535	295	
	1490	270	

[a] KBr disks. [b] Nujol mull on CsI plates.

The lack of any coordinated solvent molecule has been confirmed both by thermogravimetric measurements and by their inertness towards strong neutral ligands such as pyridine, DMSO and DMF. Their low solubility ($<10^{-3}$ mol dm^{-3}) in all the common organic solvents prevents any molecular weight measurements in solution. A laser induced vaporization mass spectrometric study of species **Ib** showed that the complex is dimeric in gas phase ($M^{\cdot +}$ at m/z 1006) [48].

The magnetic moments of **Ia** ($\mu = 1.90$ BM) and **Ib** ($\mu = 2.84$ BM) at room temperature are not diagnostic of their coordination geometries. In the case of complex **Ib**, the value found is rather low for octahedral or trigonal bipyramidal or pentagonal bipyramidal stereochemistries [49]. UV–Vis–NIR spectra of **Ib** (either in $CHCl_3$ solution or in saturated DMF solution or in Nujol mulls) show bands assignable to the Ni^{II} ions in octahedral geometry. In fact the less intense bands at 13 889 and 18 657 cm^{-1} (the ν_3 is partially obscured by intense charge-transfer absorptions) could be assigned to the ν_1 ($^3T_{2g}(F) \leftarrow {}^3A_{2g}(F)$), ν_2 ($^3T_{1g}(F) \leftarrow {}^3A_{2g}(F)$) and ν_3 ($^3T_{1g}(P) \leftarrow {}^3A_{2g}(F)$) transitions of a Ni^{II} in octahedral field [50].

*X-ray crystal structure determination of **Ib***

A view of the molecule is reported in Fig. 3 together with the atom numbering scheme. The binuclear complex has no imposed crystallographic symmetry. However a pseudo binary axis can be envisaged at the center of the rectangle formed by the nitrogen N(5) and N(15) atoms of the bridging pyridines and the Ni(1) and Ni(2) metal atoms (see Fig. 4).

The two nickel ions are at the centers of distorted octahedra. The two basal 'square' planes of the octahedrons (N(4), N(15), N(16), N(18)) about Ni(1) and (N(6), N(11), N(14), N(15)) about Ni(2) are inclined at 80.0(1)° (dihedral angle) and are connected via N(15), while the two octahedrons have in common the apex N(5). The two dapz^{2-} ligands are coordinated to nickel in the same way. Each ligand, that in principle could act as pentadentate (see Fig. 2) on a metal ion with the formation of four pentaatomic rings, is chelated with one nitrogen (N(8)) of the phthalazine moiety and one nitrogen N(6) of one hydrazonic residue on a metal ion, with formation of a pentaatomic ring. A subsequent rotation around the carbon–carbon bond adjacent to the pyridine rings (30° average value), allows the bridging of the pyridine nitrogen on the two adjacent nickel ions. A further rotation (25° average value) around the symmetrical adjacent C–C bond allows the chelation

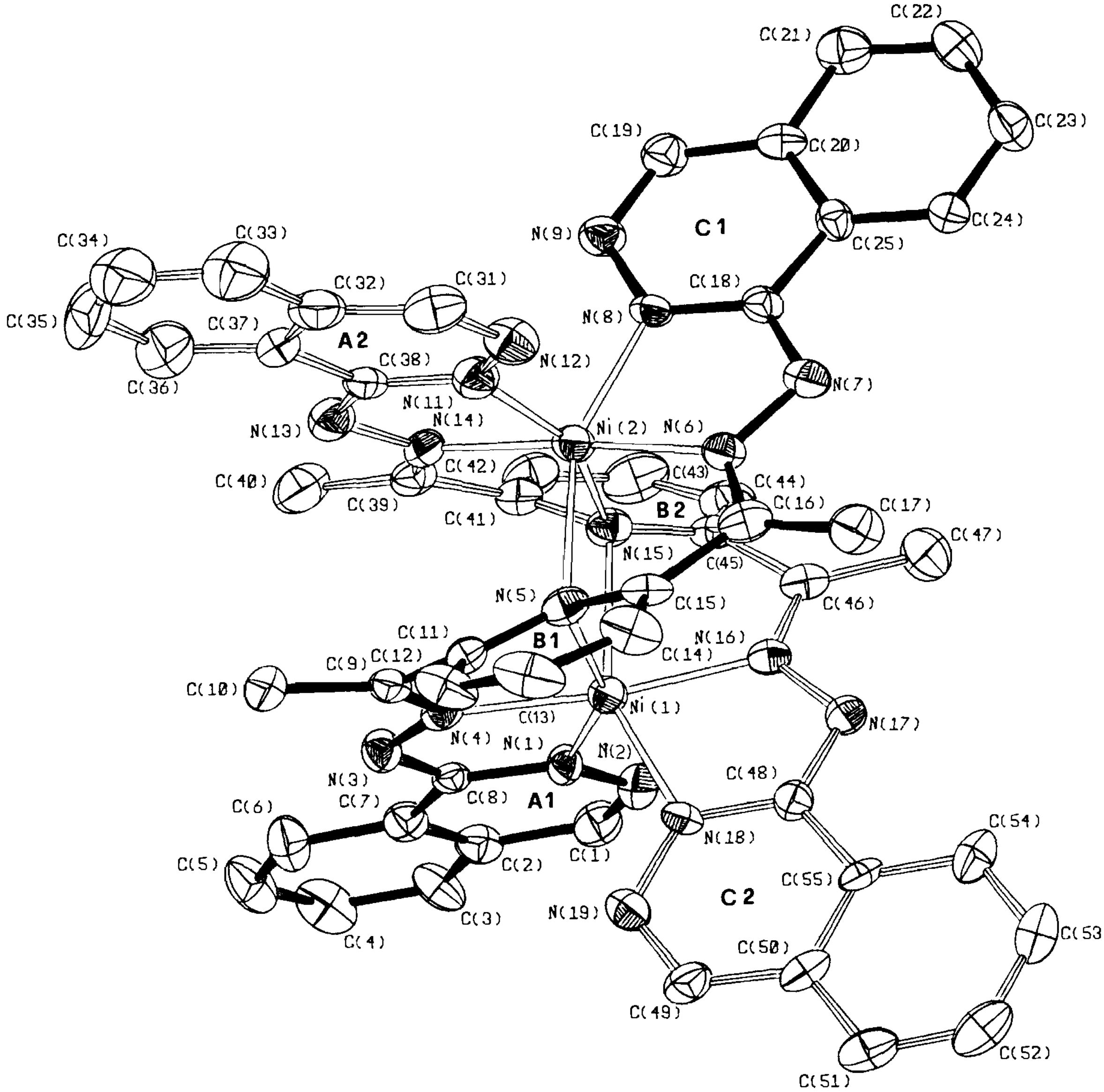

Fig. 3. An ORTEP view of the dimer **Ib** with the atom labelling. The thermal ellipsoids are drawn at the 40% probability level.

on the second nickel ion by the two nitrogens similar to the two previously described.

Fractional atomic coordinates are given in Table 4, bond lengths and bond angles in Table 5, and torsion angles in Table 6.

The Ni–N bond distances are rather different from one another. The Ni–N(diiminic) distances are 1.981 Å (average value) and Ni–N(heterocyclic) 1.999 Å. The Ni(1)–N bond distances relative to the two bridging pyridine are the longest: Ni(1)–N(5) 2.348(6) and Ni(1)–N(15) 2.347(7) Å as compared with Ni(2)–N(5) 2.313(7) and Ni(2)–N(15) 2.299(6) Å. This unexpected difference with two shorter bond distances on one Ni and two longer in the second Ni coordination sphere, could be explained with different steric hindrance of the two ligands in proximity of the two metal ions. In fact the two longer distances are associated with the higher values of the two torsion angles N(4)–C(9)–C(11)–N(5), 31(1)° and N(15)–C(45)–C(46)–N(16), 30(1)° in ligands I and II, respectively, in order to achieve the conformation suitable for Ni(1) coordination, while the two shorter Ni(2)–N bridging distances are associated with smaller torsion angles (N(5)–C(15)–C(16)–N(6), 25(1)° in ligand I and N(14)–C(39)–C(41)–N(15), 27(1)° in ligand II). The other equivalent distances in the two metal coordination spheres are exactly comparable.

An examination of the ligand bond distances shows a lack of a delocalized electron system due to the non-planar ligand conformations. The four C–N bond lengths adjacent to the pyridine ligands are 1.29(1) Å, in both ligands a value characteristic of a double C=N bond.

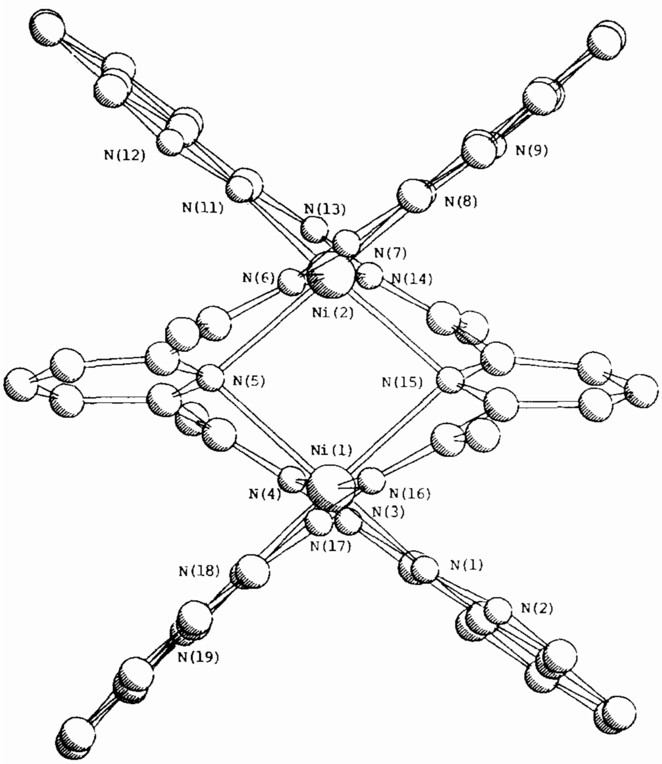

Fig. 4. View of the dimer **Ib** parallel to the Ni(1), Ni(2), N(5) and N(15) plane.

TABLE 4. Fractional atomic coordinates (×10^4) for non-hydrogen atoms and U_{eq} (Å^2×10^3) with e.s.d.s in parentheses

Atom	x	y	z	$U_{eq/iso}$[a]
Ni(1)	3033.6(5)	3284.8(5)	−474.4(9)	33.0(4)
Ni(2)	3419.0(5)	3165.6(5)	2329.4(9)	36.0(4)
N(1)	2265(3)	2946(3)	−1338(6)	32(3)
N(2)	1746(3)	3269(3)	−1649(6)	40(3)
C(1)	1256(4)	2979(4)	−2121(8)	46(4)
C(2)	1242(4)	2339(4)	−2337(8)	40(4)
C(3)	709(4)	2051(5)	−2874(8)	48(4)
C(4)	729(4)	1447(5)	−3075(9)	58(5)
C(5)	1251(5)	1115(4)	−2767(9)	59(4)
C(6)	1778(4)	1390(4)	−2252(9)	52(4)
C(7)	1775(4)	2017(4)	−2017(8)	37(3)
C(8)	2300(4)	2338(4)	−1473(7)	28(3)
N(3)	2810(3)	2035(3)	−1104(6)	38(3)
N(4)	3256(3)	2419(3)	−642(6)	33(3)
C(9)	3804(4)	2218(4)	−272(7)	37(3)
C(10)	3977(5)	1572(4)	−272(9)	52(4)
C(11)	4243(4)	2690(4)	117(7)	37(4)
C(12)	4863(4)	2662(5)	−160(8)	56(4)
C(13)	5225(4)	3166(6)	18(8)	54(4)
C(14)	4986(4)	3687(5)	479(8)	55(4)
C(15)	4377(4)	3689(4)	842(7)	38(3)
N(5)	4002(3)	3195(3)	621(6)	38(3)
C(16)	4124(4)	4190(4)	1556(8)	45(4)
C(17)	4367(5)	4817(4)	1493(9)	56(4)
N(6)	3698(3)	4015(3)	2268(6)	36(3)
N(7)	3443(3)	4430(3)	3034(6)	40(3)
C(18)	3072(4)	4142(4)	3803(7)	34(3)
N(8)	2996(3)	3530(3)	3733(6)	35(3)
N(9)	2627(3)	3218(3)	4508(6)	43(3)
C(19)	2374(4)	3523(4)	5356(8)	42(3)
C(20)	2413(4)	4160(4)	5506(8)	36(3)
C(21)	2120(4)	4463(5)	6471(8)	52(4)
C(22)	2172(4)	5077(5)	6523(9)	53(4)
C(23)	2497(4)	5409(4)	5681(9)	53(4)
C(24)	2781(4)	5115(4)	4772(8)	40(3)
C(25)	2752(4)	4492(4)	4689(8)	33(3)
N(11)	4145(3)	2738(3)	3149(6)	43(3)
N(12)	4683(4)	3005(4)	3614(7)	52(3)
C(31)	5143(5)	2649(6)	4025(9)	62(4)
C(32)	5123(5)	2016(5)	4022(9)	57(4)
C(33)	5621(5)	1655(6)	4510(11)	80(5)
C(34)	5594(6)	1045(7)	4449(11)	84(6)
C(35)	5061(7)	785(6)	3976(12)	90(6)
C(36)	4555(5)	1125(5)	3522(11)	77(5)
C(37)	4588(5)	1740(5)	3542(8)	47(4)
C(38)	4080(4)	2135(4)	3089(7)	39(3)
N(13)	3550(4)	1879(3)	2624(6)	46(3)
N(14)	3135(3)	2321(3)	2247(6)	36(3)
C(39)	2581(4)	2183(4)	1856(8)	38(3)
C(40)	2340(5)	1547(4)	1712(9)	62(4)
C(41)	2179(4)	2699(4)	1591(8)	39(4)
C(42)	1543(5)	2674(5)	1734(8)	53(4)
C(43)	1206(5)	3190(6)	1664(9)	65(4)
C(44)	1501(4)	3736(5)	1432(8)	54(4)
C(45)	2118(4)	3740(4)	1186(7)	36(3)
N(15)	2461(3)	3223(4)	1283(6)	38(3)
C(46)	2422(4)	4270(4)	682(8)	39(4)
C(47)	2235(5)	4898(4)	961(9)	60(4)
N(16)	2833(3)	4132(3)	−89(6)	33(2)
N(17)	3119(3)	4582(3)	−694(6)	36(3)
C(48)	3436(4)	4337(4)	−1591(8)	36(3)
N(18)	3455(3)	3741(3)	−1778(6)	32(2)
N(19)	3736(3)	3483(3)	−2747(6)	40(3)
C(49)	3992(4)	3837(4)	−3520(8)	44(4)
C(50)	4026(4)	4477(4)	−3386(8)	43(3)
C(51)	4313(4)	4857(5)	−4225(8)	48(4)
C(52)	4332(4)	5473(5)	−3997(11)	59(5)
C(53)	4068(4)	5734(4)	−2992(11)	57(4)
C(54)	3786(4)	5369(4)	−2177(9)	52(4)
C(55)	3754(4)	4745(4)	−2372(7)	34(3)
O(1)	9773(4)	3289(4)	7203(7)	93(2)*
O(2)	3163(4)	7079(4)	5474(8)	121(3)*
C(61)	9285(5)	3051(5)	6751(10)	78(4)*
N(21)	8804(4)	3384(4)	6367(7)	65(2)*
C(62)	8253(5)	3074(5)	5873(11)	89(4)*
C(63)	8798(6)	4018(5)	6419(12)	104(4)*
O(3)	4373(10)	−401(10)	11356(28)	125(9)*[b]
C(71)	4785(12)	−277(16)	10778(27)	136(10)*[b]
C(72)	4743(15)	−72(14)	9787(26)	114(11)*[b]

---

[a] U_{iso} is denoted by asterisk. 0.5 Population parameters is denoted by [b].

TABLE 5. Bond lengths (Å) and bond angles (°) with e.s.d.s in parentheses

Bond lengths			
Ni(1)–Ni(2)	3.125(2)	Ni(1)–N(1)	1.999(6)
Ni(1)–N(4)	1.985(7)	Ni(1)–N(5)	2.348(6)
Ni(1)–N(15)	2.347(7)	Ni(1)–N(16)	1.974(7)
Ni(1)–N(18)	2.007(7)	Ni(2)–N(5)	2.313(7)
Ni(2)–N(6)	1.975(7)	Ni(2)–N(8)	1.998(7)
Ni(2)–N(11)	1.991(7)	Ni(2)–N(14)	1.967(7)
Ni(2)–N(15)	2.299(6)	O(1)–C(61)	1.25(1)
C(61)–N(21)	1.32(1)	N(21)–C(62)	1.45(1)
N(21)–C(63)	1.40(1)	N(1)–N(2)	1.35(1)
N(1)–C(8)	1.36(1)	N(2)–C(1)	1.31(1)
C(1)–C(2)	1.43(1)	C(2)–C(3)	1.41(1)
C(2)–C(7)	1.38(1)	C(3)–C(4)	1.35(2)
C(4)–C(5)	1.37(1)	C(5)–C(6)	1.38(1)
C(6)–C(7)	1.41(1)	C(7)–C(8)	1.43(1)
C(8)–N(3)	1.33(1)	N(3)–N(4)	1.36(1)
N(4)–C(9)	1.30(1)	C(9)–C(10)	1.48(1)
C(9)–C(11)	1.45(1)	C(11)–C(12)	1.39(1)
C(11)–N(5)	1.36(1)	C(12)–C(13)	1.37(2)
C(13)–C(14)	1.37(2)	C(14)–C(15)	1.39(1)
C(15)–N(5)	1.37(1)	C(15)–C(16)	1.48(1)
C(16)–C(17)	1.49(1)	C(16)–N(6)	1.30(1)
N(6)–N(7)	1.38(1)	N(7)–C(18)	1.35(1)
C(18)–N(8)	1.37(1)	C(18)–C(25)	1.45(1)
N(8)–N(9)	1.38(1)	N(9)–C(19)	1.29(1)
C(19)–C(20)	1.42(1)	C(20)–C(21)	1.43(1)
C(20)–C(25)	1.40(1)	C(21)–C(22)	1.36(1)
C(22)–C(23)	1.40(1)	C(23)–C(24)	1.36(1)
C(24)–C(25)	1.38(1)	N(11)–N(12)	1.37(1)
N(11)–C(38)	1.34(1)	N(12)–C(31)	1.32(1)
C(31)–C(32)	1.40(2)	C(32)–C(33)	1.41(2)
C(32)–C(37)	1.38(1)	C(33)–C(34)	1.35(2)
C(34)–C(35)	1.36(2)	C(35)–C(36)	1.39(2)
C(36)–C(37)	1.36(2)	C(37)–C(38)	1.46(1)
C(38)–N(13)	1.35(1)	N(13)–N(14)	1.37(1)
N(14)–C(39)	1.28(1)	C(39)–C(40)	1.51(1)
C(39)–C(41)	1.45(1)	C(41)–C(42)	1.39(1)
C(41)–N(15)	1.36(1)	C(42)–C(43)	1.35(2)
C(43)–C(44)	1.39(2)	C(44)–C(45)	1.37(1)
C(45)–N(15)	1.36(1)	C(45)–C(46)	1.47(1)
C(46)–C(47)	1.48(1)	C(46)–N(16)	1.30(1)
N(16)–N(17)	1.36(1)	N(17)–C(48)	1.34(1)
C(48)–N(18)	1.34(1)	C(48)–C(55)	1.44(1)
N(18)–N(19)	1.37(1)	N(19)–C(49)	1.30(1)
C(49)–C(50)	1.43(1)	C(50)–C(51)	1.41(1)
C(50)–C(55)	1.41(1)	C(51)–C(52)	1.38(2)
C(52)–C(53)	1.39(2)	C(53)–C(54)	1.37(1)
C(54)–C(55)	1.40(1)		
Bond angles			
N(16)–Ni(1)–N(18)	77.8(3)	N(15)–Ni(1)–N(18)	153.2(3)
N(15)–Ni(1)–N(16)	75.4(3)	N(5)–Ni(1)–N(18)	88.5(3)
N(5)–Ni(1)–N(16)	99.9(3)	N(5)–Ni(1)–N(15)	94.5(2)
N(4)–Ni(1)–N(18)	107.3(3)	N(4)–Ni(1)–N(16)	173.0(3)
N(4)–Ni(1)–N(15)	99.3(3)	N(4)–Ni(1)–N(5)	75.7(3)
N(1)–Ni(1)–N(18)	104.8(3)	N(1)–Ni(1)–N(16)	105.6(3)
N(1)–Ni(1)–N(15)	84.1(3)	N(1)–Ni(1)–N(5)	153.1(3)
N(1)–Ni(1)–N(4)	78.1(3)	Ni(2)–Ni(1)–N(18)	129.0(2)
Ni(2)–Ni(1)–N(16)	85.4(2)	Ni(2)–Ni(1)–N(15)	47.1(2)
Ni(2)–Ni(1)–N(5)	47.4(2)	Ni(2)–Ni(1)–N(4)	87.6(2)
Ni(2)–Ni(1)–N(1)	126.1(2)	Ni(1)–Ni(2)–N(15)	48.4(2)
Ni(1)–Ni(2)–N(14)	88.4(2)	Ni(1)–Ni(2)–N(11)	129.1(2)
Ni(1)–Ni(2)–N(8)	127.4(2)	Ni(1)–Ni(2)–N(6)	87.1(2)
Ni(1)–Ni(2)–N(5)	48.4(2)	N(14)–Ni(2)–N(15)	76.2(3)
N(11)–Ni(2)–N(15)	154.8(3)	N(11)–Ni(2)–N(14)	78.6(3)
N(18)–Ni(2)–N(15)	85.3(3)	N(8)–Ni(2)–N(14)	105.2(3)
N(8)–Ni(2)–N(11)	103.5(3)	N(6)–Ni(2)–N(15)	101.3(3)
N(6)–Ni(2)–N(14)	175.5(3)	N(6)–Ni(2)–N(11)	103.6(3)
N(6)–Ni(2)–N(8)	78.3(3)	N(5)–Ni(2)–N(15)	96.8(2)
N(5)–Ni(2)–N(14)	100.0(3)	N(5)–Ni(2)–N(11)	85.5(3)
N(5)–Ni(2)–N(8)	154.5(3)	N(5)–Ni(2)–N(6)	76.4(3)
O(1)–C(61)–N(21)	121(1)	C(61)–N(21)–C(63)	124(1)
C(61)–N(21)–C(62)	117.8(9)	C(62)–N(21)–C(63)	118.5(9)

(*continued*)

TABLE 5. (*continued*)

Ni(1)–N(1)–C(8)	111.9(5)	Ni(1)–N(1)–N(2)	124.7(5)
N(1)–N(2)–C(1)	118.3(7)	N(2)–N(1)–C(8)	123.1(7)
C(1)–C(2)–C(7)	117.5(8)	N(2)–C(1)–C(2)	123.6(8)
C(3)–C(2)–C(7)	121.0(9)	C(1)–C(2)–C(3)	121.5(8)
C(3)–C(4)–C(5)	122(1)	C(2)–C(3)–C(4)	118.7(9)
C(5)–C(6)–C(7)	119.6(9)	C(4)–C(5)–C(6)	120.6(9)
C(6)–C(7)–C(8)	123.3(8)	C(2)–C(7)–C(6)	118.5(8)
N(1)–C(8)–C(7)	119.3(7)	C(2)–C(7)–C(8)	118.2(8)
N(1)–C(8)–N(3)	121.3(7)	C(7)–C(8)–N(3)	119.5(7)
Ni(1)–N(4)–N(3)	117.9(5)	C(8)–N(3)–N(4)	110.5(7)
Ni(1)–N(4)–C(9)	121.4(6)	N(3)–N(4)–C(9)	120.6(7)
N(4)–C(9)–C(10)	123.7(8)	N(4)–C(9)–C(11)	113.9(8)
C(9)–C(11)–N(5)	116.7(8)	C(10)–C(9)–C(11)	122.4(8)
C(12)–C(11)–N(5)	121.3(9)	C(9)–C(11)–C(12)	121.4(8)
C(12)–C(13)–C(14)	120.8(9)	C(11)–C(12)–C(13)	118.8(9)
C(14)–C(15)–C(16)	122.5(8)	C(13)–C(14)–C(15)	119(1)
N(5)–C(15)–C(16)	117.1(8)	C(14)–C(15)–N(5)	120.2(8)
Ni(2)–N(5)–C(15)	103.1(5)	C(11)–N(5)–C(15)	119.3(7)
Ni(1)–N(5)–C(15)	121.1(5)	Ni(2)–N(5)–C(11)	122.9(5)
Ni(1)–N(5)–Ni(2)	84.2(2)	Ni(1)–N(5)–C(11)	102.3(5)
C(15)–C(16)–C(17)	122.1(8)	C(15)–C(16)–N(6)	113.1(8)
Ni(2)–N(6)–C(16)	122.1(6)	C(17)–C(16)–N(6)	124.7(8)
Ni(2)–N(6)–N(7)	118.6(5)	C(16)–N(6)–N(7)	119.3(7)
N(7)–C(18)–C(25)	119.1(8)	N(6)–N(7)–C(18)	109.6(7)
N(8)–C(18)–C(25)	120.5(8)	N(7)–C(18)–N(8)	120.3(7)
C(18)–N(8)–N(9)	122.1(7)	Ni(2)–N(8)–C(18)	112.6(5)
N(8)–N(9)–C(19)	117.6(7)	Ni(2)–N(8)–N(9)	125.1(5)
C(19)–C(20)–C(25)	118.5(8)	N(9)–C(19)–C(20)	125.1(8)
C(21)–C(20)–C(25)	119.8(8)	C(19)–C(20)–C(21)	121.7(8)
C(21)–C(22)–C(23)	122.7(9)	C(20)–C(21)–C(22)	117.3(8)
C(23)–C(24)–C(25)	120.3(8)	C(22)–C(23)–C(24)	119.6(9)
C(18)–C(25)–C(24)	123.8(8)	C(20)–C(25)–C(24)	120.4(8)
Ni(2)–N(11)–C(38)	112.0(6)	C(18)–C(25)–C(20)	115.8(8)
N(12)–N(11)–C(38)	121.9(8)	Ni(2)–N(11)–N(12)	125.7(6)
N(12)–C(31)–C(32)	125(1)	N(11)–N(12)–C(31)	117.9(9)
C(31)–C(32)–C(33)	123(1)	C(31)–C(32)–C(37)	118(1)
C(32)–C(33)–C(34)	121(1)	C(33)–C(32)–C(37)	119(1)
C(34)–C(35)–C(36)	122(1)	C(33)–C(34)–C(35)	118(1)
C(32)–C(37)–C(36)	119(1)	C(35)–C(36)–C(37)	120(1)
C(32)–C(37)–C(38)	117.0(9)	C(36)–C(37)–C(38)	123.7(9)
C(37)–C(38)–N(13)	118.5(8)	N(11)–C(38)–C(37)	120.3(8)
C(38)–N(13)–N(14)	109.7(7)	N(11)–C(38)–N(13)	121.2(8)
N(13)–N(14)–C(39)	120.6(7)	Ni(2)–N(14)–N(13)	117.9(5)
N(14)–C(39)–C(41)	114.3(8)	Ni(2)–N(14)–C(39)	121.5(6)
C(40)–C(39)–C(41)	121.2(8)	N(14)–C(39)–C(40)	124.4(8)
C(39)–C(41)–C(42)	121.7(9)	C(39)–C(41)–N(15)	116.6(8)
C(41)–C(42)–C(43)	119(1)	C(42)–C(41)–N(15)	121.4(9)
C(43)–C(44)–C(45)	120(1)	C(42)–C(43)–C(44)	119(1)
C(44)–C(45)–N(15)	120.5(8)	C(44)–C(45)–C(46)	122.7(8)
C(41)–N(15)–C(45)	119.0(7)	N(15)–C(45)–C(46)	116.5(8)
Ni(2)–N(15)–C(41)	103.5(5)	Ni(2)–N(15)–C(45)	123.5(5)
Ni(1)–N(15)–C(41)	121.2(5)	Ni(1)–N(15)–C(45)	101.5(5)
C(45)–C(46)–N(16)	113.3(8)	Ni(1)–N(15)–Ni(2)	84.5(2)
C(47)–C(46)–N(16)	123.9(8)	C(45)–C(46)–C(47)	122.6(8)
C(46)–N(16)–N(17)	119.4(7)	Ni(1)–N(16)–C(46)	121.9(6)
N(16)–N(17)–C(48)	108.9(7)	Ni(1)–N(16)–N(17)	118.6(5)
N(17)–C(48)–N(18)	122.1(7)	N(17)–C(48)–C(55)	117.5(8)
Ni(1)–N(18)–C(48)	111.6(5)	N(18)–C(48)–C(55)	120.4(8)
Ni(1)–N(18)–N(19)	125.3(5)	C(48)–N(18)–N(19)	123.1(7)
N(19)–C(49)–C(50)	123.6(8)	N(18)–N(19)–C(49)	118.4(7)
C(49)–C(50)–C(51)	123.1(8)	C(49)–C(50)–C(55)	118.4(8)
C(50)–C(51)–C(52)	118.6(8)	C(51)–C(50)–C(55)	118.4(8)
C(52)–C(53)–C(54)	119.1(9)	C(51)–C(52)–C(53)	123(1)
C(50)–C(55)–C(54)	121.0(8)	C(53)–C(54)–C(55)	120.2(9)
C(48)–C(55)–C(50)	115.8(8)	C(48)–C(55)–C(54)	123.2(8)

The conformations of ligands I and II can be defined by the torsion angles given in Table 6 and by the values of the dihedral angles between the different planes (for nomenclature of the planes see Fig. 3).

TABLE 6. Selected torsion angles in the L ligands

I		II	
C(7)–C(8)–N(3)–N(4)	178.8(7)	C(37)–C(38)–N(13)–N(14)	−179.7(8)
C(8)–N(3)–N(4)–C(9)	−177.2(8)	C(38)–N(13)–N(14)–C(39)	−174.9(8)
N(3)–N(4)–C(9)–C(11)	175.8(7)	N(13)–N(14)–C(39)–C(41)	174.9(7)
N(4)–C(9)–C(11)–N(5)	31(1)	N(14)–C(39)–C(41)–N(15)	27(1)
C(9)–C(11)–N(5)–C(15)	−170.7(8)	C(39)–C(41)–N(15)–C(45)	−171.4(8)
C(16)–C(15)–N(5)–C(11)	−171.2(8)	C(46)–C(45)–N(15)–C(41)	−171.6(8)
N(5)–C(15)–C(16)–N(6)	25(1)	N(15)–C(45)–C(46)–N(16)	30(1)
C(15)–C(16)–N(6)–N(7)	176.7(7)	C(45)–C(46)–N(16)–N(17)	175.3(7)
C(16)–N(6)–N(7)–C(18)	−172.2(8)	C(46)–N(16)–N(17)–C(48)	−169.0(8)
N(6)–N(7)–C(18)–C(25)	−179.8(7)	N(16)–N(17)–C(48)–C(55)	177.7(7)

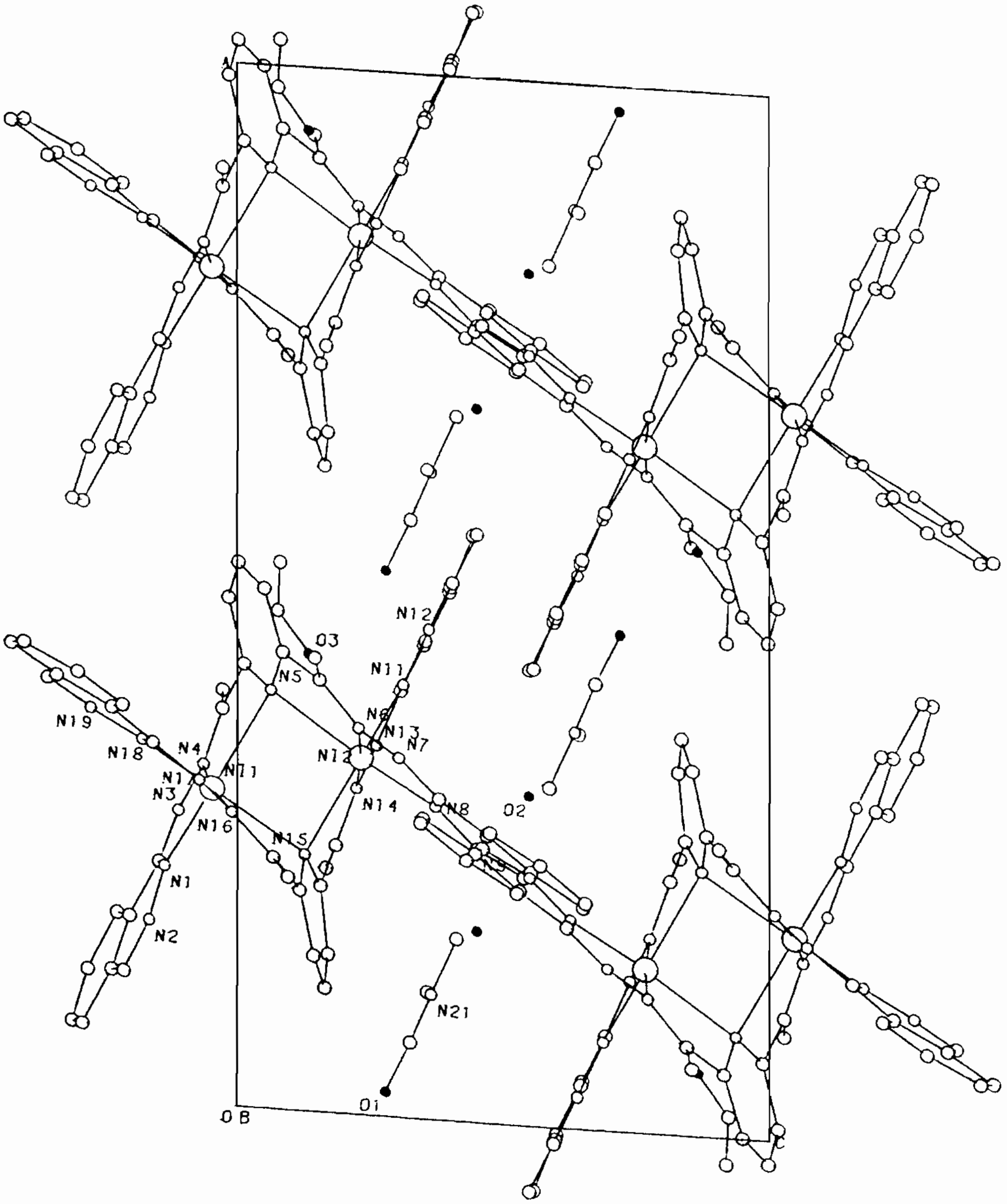

Fig. 5. The unit cell content as viewed along the *b* crystallographic axis. (The ethanol molecules are statistically distributed (50%) among the four crystallographic positions here indicated, for sake of clarity the carbon labelling is omitted.)

A1∧B1	36.6(2)°	B1∧C1	39.2(2)°	A1∧C1	73.4(2)°
B2∧A2	34.6(2)°	C2∧B2	49.9(2)°	A2∧C2	81.3(2)°
A1∧A2	9.4(2)°	B1∧B2	29.4(3)°	C1∧C2	4.9(1)°

While the bicyclic rings of each dapz^{2-} ligand anions tend to be parallel to the corresponding ring in the second ligand anion (A1∧A2 9.4° and C1∧C2 4.9°), the two pyridine rings are inclined at 29.4°. The other values of the dihedral angles show different conformations of the two ligands which are reflected in the reported differences in the bridging distances and angles. The angles to Ni(1) and Ni(2) with the nitrogens of the bridging pyridines N(5)–Ni(1)–N(15) and N(5)–Ni(2)–N(15) are 94.5(3) and 96.8(2)°, respectively, while Ni(1)–N(5)–Ni(2) and Ni(1)–N(15)–Ni(2) are 84.2(2) and 84.5(2)°, respectively. A dimeric zinc derivative with the ligand 2,6-diacetylpyridine-bis(2′-pyridylhydrazone)(H_2dapp), has been reported [51], i.e. [Zndapp]$_2$ 2CHCl$_3$·2H$_2$O, where the dapp ligand differs from our dapz, due to the presence of pyridine moieties in place of phthalazine. The two structures are characterized by a similar arrangement of the nitrogen donor atoms around the metal ions, including the bridging pyridines. The distorted octahedral dimer [dappZn]$_2$ is characterized by a crystallographically imposed two fold axis symmetry and consequently the noticed asymmetry in the two Zn–N(py) distances, which differ by 0.20 Å, is the same for each Zn ion.

A further example of bridging pyridines in dimeric complexes is shown by Cu$_2$[2,6-di(2′-methoxyethyliminomethyl-pyridine)][ClO$_4$]$_2$·H$_2$O [52], where the bridges between the metal centers are asymmetric: the Cu–N(py) distances are shorter around one metal ion with respect to the second one, but in this case this is related also to the different coordination numbers around the two metal centers (*CN* = 7 where the Cu–N(py) are longer and *CN* = 5 where they are shorter). With the protonated H_2dapp ligand the $[M(H_2dapp)(H_2O)]^{2+}2Cl^-$ (M = Zn, Co) complexes are also known. They are isomorphous and have pentagonal bipyramidal geometries with H_2dapp forming the equatorial plane and the water molecules in axial positions. The dimeric zinc–dapp complex, is centrosymmetric, while this symmetry is no longer maintained with the more bulky ligand dapz^{2-}.

The torsion angles around the C–C bond adjacent to the pyridine ring are 32.6 and 29.2°, respectively, in dapp^{2-} while in dapz^{2-} they are somewhat different, 30 and 25°. The C–C and C–N bond distances in the pyridine rings and the various C–C, C–N and N–N distances in the side chains appear comparable with those of H_2dapp and dapp^{2-}.

The packing diagram of complex **Ib** is shown in Fig. 5. DMF molecules together with disordered ethanol molecules are clathrated in the structure without significant interaction between them and with the dimer; while the water molecules crystallized in the structure form contacts with nitrogens not involved in the metal coordination (N(9)...O(2) 3.04(1) Å).

It becomes rather evident that the ligand geometry constraints are not the only factors influencing the encountered differences but the electronic factors play a relevant role. In fact the difference of the bond distances between the carbon bearing the diimine group and pyridine nitrogen in the case of [dappZn]$_2$ dimer (average 1.318 Å, sp^2 nitrogen) as compared with those of the carbon bearing the diimine group and the α-phthalazine nitrogen in the case of [dapzNi]$_2$ (average 1.35 Å) suggests, in the second case, the presence of a sp^3 hybridized nitrogen. This conclusion is also supported by the angles centered on the nitrogen atoms of this kind relative to the four phthalazine residues.

As far as the low magnetic moment of **Ib** ($\mu = 2.84$ BM) is concerned, an antiferromagnetic coupling between the two Ni^{II} ions cannot be ruled out. Some preliminary measurements at low temperatures (up to 70 K) indicate that the magnetic behaviour of **Ib** does not follow the Curie–Weiss law. The observed (χ_M) susceptibilities and magnetic effective moments (μ)* of the complex **Ib** are reported in Fig. 6. Magnetic parameters are derived from least-squares fitting (see equation in footnote that provides the calculated susceptibilities, χ_{calc}) corrected for the susceptibilities (χ_{param}) of possible paramagnetic impurity and taking into account temperature-independent paramagnetism (*TIP*).

The best fitting values are $g = 2.20$, $J = -32.7$ (antiferromagnetic); the g value is within the usual range [53]; the absolute value of J is quite high with respect to complexes of analogous ligands and geometry; Ni(1), N(15), Ni(2) and N(5) form a planar system, where both Ni(1)–N(15)–Ni(2) and Ni(1)–N(5)–Ni(2) bond angles are 84.5 and 84.2°, respectively (see crystal and molecular structure). In spite of the large Ni–Ni distance (3.125 Å) the pyridine nitrogens N(5) and N(15) provide a very efficient superexchange mechanism when compared with other ligands that provide bridging nitrogen atoms [54, 55]. The amount of paramagnetic impurity is negligible within the experimental errors. Due to high χ values over the whole temperature range, introduction of different *TIP* values within the usual range does not significantly affect the fitting.

---

*$\mu = 2.828[(\chi_M - \chi_D)T]^{1/2}$ BM; $\chi_M = 2\chi_A$; χ_D represents the diamagnetic correction [46]; $\chi_M = \chi_{calc} = (1-\rho)(6 \times 0.1251 g^2)/[T(5+3f^2+f^3)/(5+f^2)] + TIP + \rho\chi_{param}$; $f = \exp(2J/kT)$ [53]. The best-fitting values of the parameters are obtained by minimizing the function $F = \Sigma_N(\chi_{obs} - \chi_{calc})^2$, where N is the number of measurements at different T. The F/N value, taken as a gauge of agreement between calculated and experimental values is small, when compared with actual experimental errors.

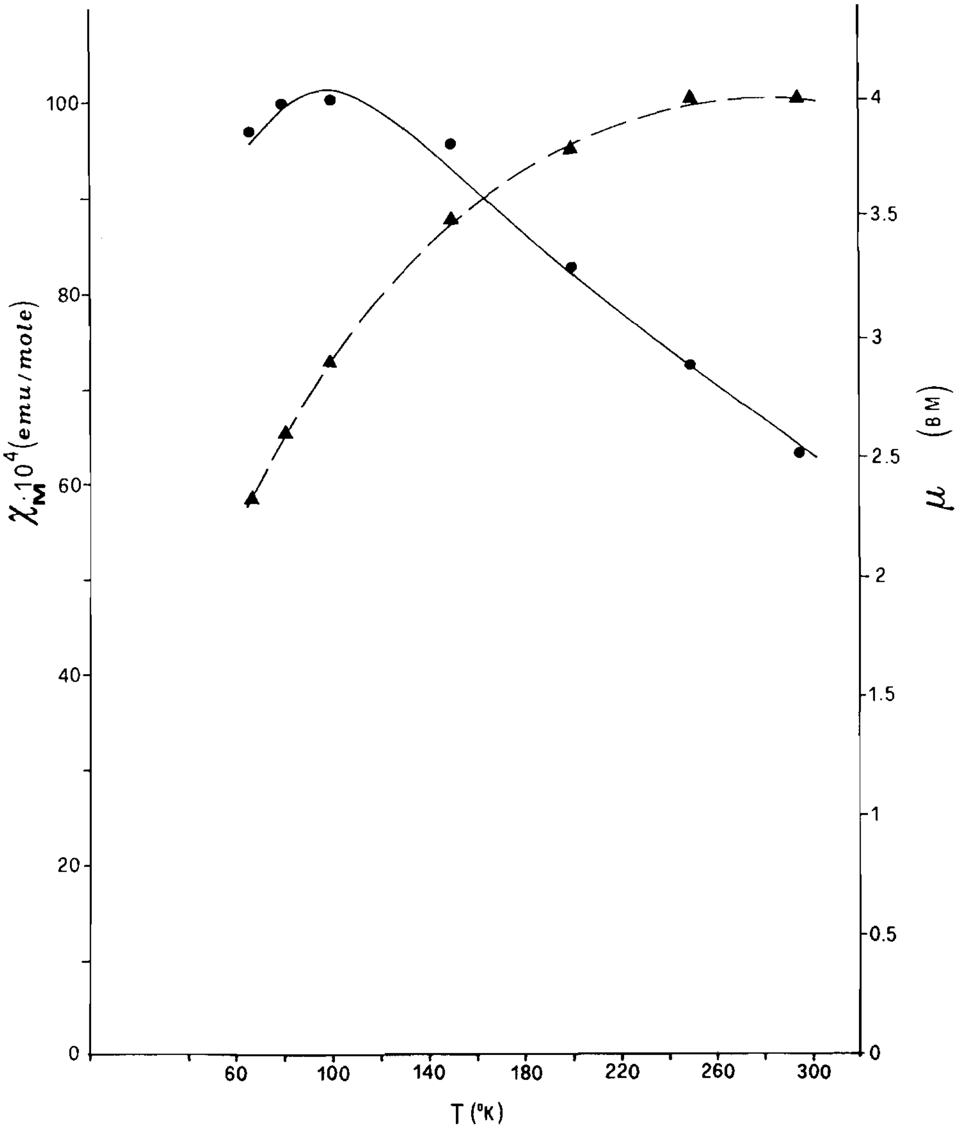

Fig. 6. Observed magnetic susceptibility χ_M (●) and effective magnetic moment μ (▲) vs. temperature for **Ib**. The solid line represents the calculated susceptibilities.

In complexes **I**, the presence of the ligand in the bisdeprotonated form has been confirmed by their reactivity (**Ia** and **Ib**) towards HCl and $HClO_4$. While in ethanolic solution, complexes **Ia** and **Ib** undergo, step by step, mono- and bisprotonation by HCl to the corresponding **III** and **II** species, respectively, by using $HClO_4$ only monoprotonation to species **V** is achieved (either in molar ratios 1:1 or 1:2). By reacting **Ia** and **Ib** species with an excess of the acids the protonated ligand $[H_4L][X]_2$ is quantitatively isolated.

Adducts $[H_2LMCl_2]_x$ *(IIa–e)*

By carrying out the reaction of the ligand and Cu^{II}, Ni^{II} and Zn^{II} chlorides in molar ratio 1:1, the corresponding adducts (**IIa, IIb** and **IIc**) are obtained, which, except **IIb**, are all non-conducting in $CHCl_3$, but electrolytes 1:2 in MeOH (due to the deprotonation of the corresponding 10^{-3} M methanolic solutions by MeOH to **I** species as confirmed by their UV–Vis spectra). Tables 7 and 8 summarize the analytical and physicochemical data of the obtained adducts.

Their IR spectra (KBr pellets) show the presence of the ν(NH) band shifted by coordination to the metal ion of the adjacent (C=N hydrazonic group to 3210 (**IIa**), 3240 (**IIb**) and 3250 (**IIc**) cm^{-1}, together with some other shifted bands in the region 1400–1000 cm^{-1} probably due to coordinated (coordinated pyridine at 1016 cm^{-1} for **IIc**) phthalazine systems. Thermogravimetric measurements indicate that compounds **IIa** and **IIc** do not contain coordinated solvent molecules, while two coordinated water molecules are present in

TABLE 7. Analytical and physicochemical data of species **II**

Complex	Color (yield (%))	Elemental analysis						μ[a]	Electronic spectra[b]	
			C	H	N	Cl	M		(cm^{-1})	ϵ
$\{[H_2LCuCl_2]\}_2$ **(IIa)**	dark brown (92)	Found	51.55	3.60	21.95	12.15	10.70	1.90	36765	27366
									34483	22633
									32468	21811
		Calc. for $C_{50}H_{42}N_{18}Cu_2Cl_4$	51.57	3.64	21.67	12.19	10.92		24876	24691
									22321	11207
									19231	3025
									16779	1078
									14706	517
									13158	388
$\{[H_2LNi\cdot 2H_2O][2Cl]]_2$ **(IIb)**	dark green (90)	Found	50.90	4.00	20.50	11.10	9.30	2.42[c]	37037	23897
									30120	16432
									23810	12500
		Calc. for $C_{50}H_{50}N_{18}Ni_2Cl_4O_4$	50.44	3.87	21.19	11.94	9.87		18231	2548
									16666	1748
									15151	1548
									14124	1451
$[H_2LZnCl_2]$ **(IIc)**	yellow–orange (85)	Found	51.60	3.70	21.30	12.30	11.90		38461	22347
									29070	26845
		Calc. for $C_{25}H_{21}N_9ZnCl_2$	51.41	3.63	21.60	12.15	11.20		26042	26850
									23148	1006
$\{[H_2LNi\cdot 2DMF][2Cl]\}_2$ **(IId)**	dark brown	Found	51.75	4.95	21.80	9.65	8.35	3.22		
		Calc. for $C_{31}H_{35}N_{11}NiCl_2O_2$	51.48	4.87	21.30	9.80	8.11			
$\{[H_2LNi\cdot 2DMSO][2Cl]\}_2$ **(IIe)**	dark brown	Found	47.85	4.50	17.50	10.25	8.95	3.28		
		Calc. for $C_{58}H_{66}N_{18}Cl_4Ni_2S_4O_4$	47.50	4.53	17.19	9.67	8.74			

[a] At room temperature. [b] In chloroform solution. [c] Containing 5% of the diamagnetic compound **IIIb**.

complex **IIb**. In fact **IIb** easily exchanges the two coordinated water molecules by reaction with DMSO and DMF (**IId** and **IIe**, respectively). As far as the position of the metal ions (compartments A or B) is concerned, the IR data strongly support coordination into compartment A. The solubility of **IIc** in $CHCl_3$ allows reproducible molecular weight measurements indicating that the complex is monomeric (calc. 583.4; experimental 596). An X-ray structural determination of **IIc** shows that the metal is coordinated into compartment A with distorted trigonal bipyramidal geometry [56].

The very low solubilities of **IIa** and **IIc** prevent any molecular weight measurements, but on the basis of their spectroscopic data, suggesting for them an octahedral geometry, the dimeric nature of the two complexes cannot be excluded (cf. Scheme 2).

It is noteworthy that **IIb** is normally contaminated by variable amounts (5–10% when the reaction is carried according to the conditions reported in 'Experimental') of the monodeprotonated species **IIIb**, due to a partial monodeprotonation of **IIb** by the alcohol. In fact, in dilute alcoholic solutions (either ethanol or methanol) **IIb** undergoes monodeprotonation to **IIIb**, also in anhydrous conditions and under inert atmosphere, proving that the alcohol acts as the deprotonating agent. The ability of the solvent to deprotonate the ligand is due to the highly increased acidity of the hydrazonic hydrogens caused by coordination of the adjacent groups with the transition metal. It is known, in fact, that coordination to transition metals may increase the acid dissociation constant of some hydrazone systems by a factor of 10^5–10^8 [47, 57]. The presence, in monodeprotonated species, of a M–N σ-bond, lowers the effective nuclear charge of the metal ion, thus lowering the dissociation constant of the hydrazonic hydrogen residue, which cannot be further deprotonated by the solvent and requires the use of a stronger base (Proton Sponge).

Monodeprotonated species [HLMCl]$_x$ (IIIa and IIIb)

By reacting either **IIa** or **IIb** with Proton Sponge (*N*,*N*,*N*′,*N*′-tetramethyl-1,8-diaminonaphthalene), a strong non-coordinating base, in molar ratio 1:1, the same monodeprotonated species (**IIIa** and **IIIb**) as obtained by monoprotonation of **Ia** and **Ib** with HCl

TABLE 8. Main IR bands characteristic of species **II** (cm^{-1})

Complex	C=C, C=N[a] (pyridine and phthalazine)	Pyridine ring breathing	ν(M–N)[b]	ν(M–Cl)[b]
IIa	1616 1602 1590 1520	1000	365 335 315 270	308
IIb	1602 1590 1550 1520	1000	350 310 290 270	
IIc	1615 1610 1590 1530 1500	1016	350 305 270	325 265
IId	1607 1590 1540 1510	1000		
IIe	1610 1595 1545 1528	1000		

[a] KBr disks. [b] Nujol mull on CsI plates.

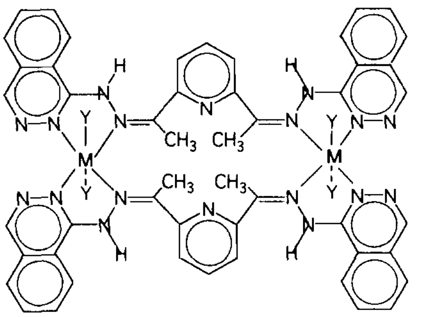

Y = H_2O, DMF, DMSO = IIb, IId, IIe (x 4 Cl-)

Y = Cl = IIa

Scheme 2.

are formed. **IIIa** and **IIIb** were also quantitatively obtained by direct reaction of the ligand and metal chlorides in ethanol/pyridine mixture, as solvent. Finally, by reaction of either **IIa** or **IIb** with Proton Sponge in molar ratio 1:2, **Ia** or **Ib** were quantitatively obtained, thus confirming the sequence:

$$\begin{tikzcd} {[\mathrm{H_2dapzMCl}]_x} \arrow[r, shift left, "+B; -BH"] \arrow[rr, bend left=40, "-2H^+"] & {[\mathrm{HdapzMCl}]_x} \arrow[l, shift left, "+H^+"] \arrow[r, shift left, "+B; -BH"] & {[\mathrm{dapzM}]_x} \arrow[l, shift left, "+H^+"] \arrow[ll, bend right=30, "+2H^+"'] \end{tikzcd}$$

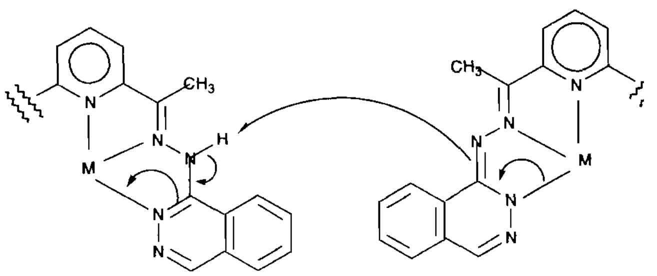

Scheme 3.

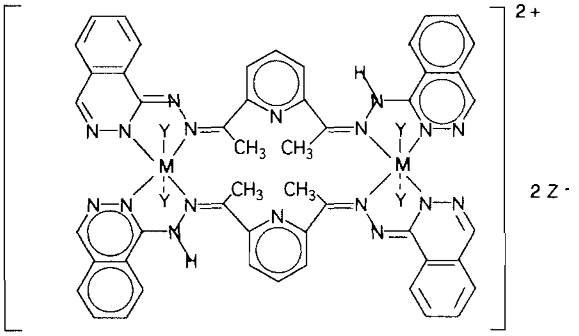

Y = H_2O; Z = Cl; M = Cu = IIIa

Y = H_2O; Z = ClO_4; M = Cu = Va

Y = absent; Z = Cl; M = Ni = IIIb

Y = absent; Z = ClO_4; M = Ni = Vb

Scheme 4.

IIIa and **IIIb** can be isolated also by reaction of equimolar amounts of **I** and **II** species in dichloromethane at room temperature. In this case, compounds **I** acts as base in deprotonating compounds **II**, thereby achieving an increase in the aromaticity of its phthalazine rings (Scheme 3).

The IR spectra of **IIIa** and **IIIb** are characterized by the presence of a medium band at 3240 (**IIIa**) and 3220 (**IIIb**) cm^{-1} (anhydrous Nujol) due to the ν(NH). In the range 1600–1300 cm^{-1} the bands characteristic either of **I** and **II** species are present in addition to a new intense band at 1390 cm^{-1} together with two other medium bands at 1420 and 1380 cm^{-1}, respectively, due to ring vibrations of the coordinated phthalazine. Moreover the lack of the band at 1020 cm^{-1} (coordinated pyridine), present either in **I** and **II** species, suggests that the pyridine nitrogen does not participate in the coordination.

That **IIIb** is diamagnetic clearly indicates a square planar stereochemistry of the Ni^{II} complex, as confirmed by the presence in its electronic spectrum ($CHCl_3$) of a broad band centred at 14 925 cm^{-1}. Since **IIIa** and **IIIb** show similar IR and UV–Vis spectra, the same geometry could be tentatively assigned also to **IIIa** ($\mu = 1.85$ BM).

The low solubilities of **IIIa** and **IIIb** in the common aprotic solvents prevent the measurement of conductances and the estimation of molecular weights. Nevertheless, their reactivity towards acids and bases is

TABLE 9. Analytical and physicochemical data of species **III**

Complex	Color (yield (%))	Elemental analysis						μ^a	Electronic spectra^a	
			C	H	N	Cl	M		(cm^{-1})	ϵ
$\{[HLCu\cdot 2H_2O][2Cl]\}_2$ (**IIIa**)	red–brown (80)	Found	51.15	3.60	21.50	6.15	10.35	1.85	36496	32538
									34247	33623
									28571	21258
		Calc. for	51.63	4.13	21.68	6.11	10.93		23810	32104
		$C_{50}H_{48}N_{18}Cl_2O_4$							15625	875
$\{[HLNi][Cl]\}_2$ (**IIIb**)	dark brown (75)	Found	53.85	4.40	21.60	6.10	10.10		37873	45253
									31250	29294
		Calc. for	53.75	3.97	22.56	6.35	10.51		26042	44253
		$C_{50}H_{40}N_{18}Cl_2Ni_2$							23809	25554
									22727	17451
									21186	12153
									19380	4986
									16666	2361
									15432	2099
									14925	1836

[a]At room temperature. [b]In chloroform solution.

TABLE 10. Main IR characteristic bands of species **III** (cm^{-1})

Complex	C=C, C=N^a (pyridine and phthalazine)	Pyridine ring breathing	ν(M–N)^b	ν(M–Cl)^b
IIIa	1600	990	388	310
	1580		345	
	1550		322	
	1510		268	
	1420			
	1390			
IIIb	1595	990	320	
	1582		288	
	1540		270	
	1510			
	1420			
	1390			

[a]KBr disks. [b]Nujol mull on CsI plates.

consistent with the dimeric structure postulated (Scheme 4).

Moreover both species **II** and **III** show in MeOH, DMF and acetonitrile solutions, UV–Vis spectra completely different from those of the same species in chloroform or dichloromethane solutions. In protic solvents, in fact, both species **II** and **III** tend to undergo successive deprotonation reactions to the corresponding species **I**. Probably different deprotonation and protonation equilibria are present that are hard to interpret. Kinetic information about the protonation of **I** and the deprotonation of **II** and **III** would assist in interpreting the equilibria involved. Accordingly, spectrophotometric measurements were attempted, but the data did not lead to acceptable results (Tables 9 and 10).

Mononuclear perchlorates $[(H_2L)_2M][ClO_4]_2$ *(IVa and IVb)*

By reacting the ligand with Cu^{II} and Ni^{II} perchlorates in molar ratio 2:1 in EtOH, compounds **IVa** and **IVb** are obtained in high yields. Tables 11 and 12 summarize the analytical and physicochemical data of **IVa** and **IVb**. The analytical data are in agreement with a formulation $[(H_2L)_2M][ClO_4]_2$, where the metal ions are bridging two ligand entities through the terminal phthalazine nitrogens. In fact their IR spectra are characterized by the presence of the ν(N–H) stretching band at the same wavenumber as in the free ligand (3340 cm^{-1}) and the bands in the region 1600–1500 cm^{-1} are unchanged relative to the free ligand, as expected for a coordination in compartment B, while some phthalazine bands (1400–1200 cm^{-1}) appear shifted. Due to their low solubilities in the common organic solvents, where they are stable, conductometric measurements on **IVa** and **IVb** are prevented. As far as the stereochemistry of the two molecules is concerned, the presence in **IVa** (μ=1.85 BM) of two coordinated water molecules, as confirmed by thermogravimetric measurements and exchange reactions with strong neutral ligands (Py, DMSO, DMF) suggests an octahedral geometry, while the square planar geometry must be invoked for **IVb** due to its diamagnetism. The electronic spectrum of **IVb** ($CHCl_3$) shows a broad band centered at 14 164 cm^{-1}, while in the case of complex **IVa** two weak broad bands are present at 13 021 and 11 765 cm^{-1}, respectively, in good agreement with the literature data relative to Ni^{II} and Cu^{II} complexes with the proposed stereochemistries. In addition, both species **IVa** and **IVb** do not react with Proton Sponge to form deprotonated species, thus confirming that the metal

TABLE 11. Analytical and physicochemical data of species **IV**

Complex	Color (yield (%))	Elemental analysis						μ^a	Electronic spectra^b	
			C	H	N	Cl	M		(cm^{-1})	ϵ
$[(H_2L)_2Cu \cdot 2H_2O][ClO_4]_2$ (**IVa**)	brown (85)	Found	50.25	3.60	21.15	5.70	6.10	1.85	36232	17360
									34247	17902
									26316	26582
		Calc. for $C_{50}H_{47}N_{18}Cl_2CuO_{10}$	50.30	3.89	21.13	5.94	6.33		20352	5244
									15625	136
									13021	105
									11765	84
$[(H_2L)_2Ni][ClO_4]_2$ (**IVb**)	dark brown (90)	Found	51.80	3.50	21.85	5.90	5.10		36765	28785
									34722	26013
									26882	31130
		Calc. for $C_{50}H_{42}N_{18}Cl_2NiO_8$	52.08	3.67	21.88	6.15	5.16		15923	290
									14164	153
									12019	105

[a] At room temperature. [b] In chloroform solution.

TABLE 12. Main IR characteristic bands of species **IV** (cm^{-1})

Complex	ν(NH)	C=C, C=N^a (pyridine and phthalazine)	Pyridine ring breathing	ν(M–N)^b	$\nu(ClO_4^-)$
IVa	3340	1610	990	368	1095
		1595		350	
		1560		320	
		1535		270	
IVb	3340	1610	995	370	1100
		1590		346	
		1550		315	
		1520		288	
				270	

[a] KBr disks. [b] Nujol mull on CsI plates.

ion is coordinated far from the hydrazonic protons (i.e. in compartment B) (Scheme 5).

It is noteworthy that in the case of nickel(II) and copper(II) perchlorates, the metal is selectively present in the coordination compartment B of the ligand, while in the case of the same metal chlorides only complexes with the metal in the coordination compartment A are obtained.

Monodeprotonated perchlorates $\{[HLM][ClO_4]\}_x$ *(**Va** and **Vb**)*

Unlike the metal chlorides, the reaction between metal perchlorates and the ligand in molar ratio 1:1 does not afford simple adducts, such as compounds **II**, but monodeprotonated species $[HLM][ClO_4]$ (M = Cu, **Va**; Ni, **Vb**), analogous to compounds **III**, whose analytical and physicochemical data are collected in Tables 13 and 14.

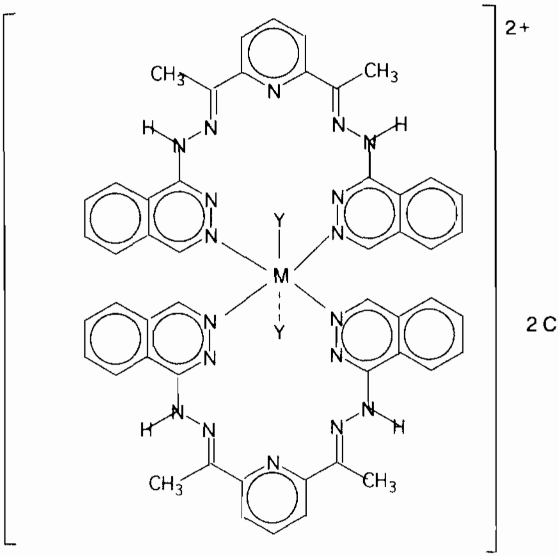

Y = H_2O; M = Cu = IVa

Y = absent; M = Ni = IVb

Scheme 5.

This behaviour, indicating an inversion of the choice of the coordination compartment depending only on the molar ratios of the reagents (2:1→**IV**, metal in compartment B; 1:1→**V**, metal in compartment A), is rather puzzling. It might be that the reaction in molar ratio 1:1 starts with the formation of the more stable species **IV**; then, due to the presence of metal perchlorate in excess for the stoichiometry of these products, a second metal ion enters into one of the A compartments of the two ligand molecules present in complexes **IV**. This behaviour of the second metal ion probably causes a consistent distortion of the ligand

TABLE 13. Analytical and physicochemical data of species **V**

Complex	Color (yield (%))	Elemental analysis	C	H	N	Cl	M	μ^a	Electronic spectra^b (cm^{-1})	ϵ
$\{[HLCu\cdot 2H_2O][ClO_4]\}_2$ (**Va**)	red–brown	Found	46.20	3.35	19.10	6.00	10.00	1.85	37593	53595
	(85)								34247	47712
		Calc. for	46.52	3.74	19.53	5.94	9.85		27173	35947
		$C_{50}H_{48}N_{18}Cl_2Cu_2O_{12}$							24875	42156
									19841	15032
$\{[HLNi][ClO_4]\}_2$ (**Vb**)	brown	Found	49.20	3.25	20.20	6.30	9.00		37317	32076
	(90)								29762	26124
		Calc. for	49.66	3.33	20.85	5.86	9.71		26882	29100
		$C_{50}H_{40}N_{18}Cl_2Ni_2O_8$							24876	17195
									22936	9920
									19841	2314
									15151	992
									14124	826

[a]At room temperature. [b]In chloroform solution.

TABLE 14. Main IR characteristic bands of species **V** (cm^{-1})

Complex	ν(NH)	C=C, C=N^a (pyridine and phthalazine)	Pyridine ring breathing	ν(M–N)^b	$\nu(ClO_4^-)$
Va	3290 b	1620	995	310	1095
		1590			
		1560			
		1530			
		1490			
Vb	3290 b	1620	995	318	1095
		1590			
		1550			
		1520			

[a]KBr disks. [b]Nujol mull on CsI plates.

and consequently the loss of the metal ion from compartment B, followed by its rearrangement into compartment A of the second ligand molecule. This affords a dimeric molecule of $\{[H_2dapzM][ClO_4]_2\}_2$. Under the reaction conditions, however, the hydrazonic hydrogens are acidic enough, due to the coordination of the adjacent C=N groups to the metal, to be deprotonated by the solvent to give the final products $\{[HdapzM][ClO_4]\}_2$ (see Scheme 4). The quantitative isolation of **V** species by reacting, in absolute ethanol, either **IVa** or **IVb** with the corresponding metal perchlorate (either in molar ratio 1:1 or 1:5), seems to be in agreement with the proposed mechanism.

The same complexes **Va** and **Vb** are obtained by reacting the ligand and metal perchlorates in molar ratio 1:1 in a mixture ethanol:pyridine (2:1, vol.:vol.) as solvent.

Unlike compounds **IV**, both **Va** and **Vb** species undergo deprotonation to **Ia** and **Ib**, respectively, by Proton Sponge (c.f. **IIIa** and **IIIb** species), thus suggesting metal coordination into compartment A, and their dimeric nature.

The IR spectra of **Va** and **Vb** are characterized by the presence of a medium intense band at 3290 cm^{-1} due to ν(NH) shifted, with respect to the free ligand, as a consequence of the coordination of the adjacent imino group (see complexes **II** and **III**). In the range 1650–1400 cm^{-1}, in addition to the bands at 1590 and 1490 cm^{-1} typical of species **I**, the compounds **Va** and **Vb** show a band at 1620 cm^{-1} due to the uncoordinated phthalazine (see the free ligand). In addition, the bands that in the free ligand fall at 1560 and 1540 cm^{-1}, appear shifted at 1560 and 1530 cm^{-1} (**Va**) and 1550 and 1520 cm^{-1} (**Vb**), and could be assigned to the two different C=N coordinated to the metal ion. The characteristic strong band of perchlorate ion is present at 1095 cm^{-1}. As far as the stereochemistry of **Va** and **Vb** is concerned, the diamagnetism of **Vb** clearly suggests a square planar geometry around the nickel(II) ion. The presence in **Va** of two coordinated water molecules suggests an octahedrally coordinated copper(II) ion. The latter geometry is in good agreement with the observed magnetic moment (μ=1.85 BM). In the absence of molecular weight measurements the dimeric nature of these species cannot be ruled out, and the proposed geometry could be obtained by coordination with the hydrazonic groups of two different molecules of the monodeprotonated ligand.

Conclusions

The interaction of the new ligand H_2dapz with some transition metal salts suggests the following considerations.

(i) Depending on the reaction conditions (in the case of zinc salts) the metal ions can be selectively coordinated into one of the two compartments.

(ii) The species where the metal ions are coordinated into compartment A (i.e. **I**, **II**, **III**, **V**) could be used to synthesize either homo- or heterobinuclear species [58] due to the presence of the two uncoordinated phthalazine nitrogens in a suitable position.

(iii) In species **I**, the presence of the ligand in the bisanionic form suggests a possible strong stabilizing effect of the ligand towards the metal ion in low oxidation states, possibly making them good catalysts in reactions involving organometallic intermediates (**Ib** in cross-coupling reactions). Preliminary results on the catalytic activity of **Ib** and some polynuclear species (Ni–Ni; Ni–Pd–Ni) in the cross coupling reactions Csp^3–Csp^2 (n-butyl magnesium chloride and bromobenzene) have been reported [59].

(iv) The ligand shows a high tendency to form dimeric species due to the possibility of free rotation of the pyridine side chains around the C–C single bonds.

Acknowledgement

The technical assistance of Mr F. De Zuane, for magnetic data collection, is gratefully acknowledged.

References

1 J. C. Bailar, Jr., *Coord. Chem. Rev., 31* (1980) 53.
2 R. Lontie and L. Vanquickenborne, in H. Sigel (ed.), *Metal Ions in Biological Systems,* Vol. 3, Marcel Dekker, New York, 1974.
3 J. A. Fee, *Struct. Bonding (Berlin), 23* (1975) 1.
4 W. H. Vanneste and A. Zuberbuehler, in O. Hayaishi (ed.), *Molecular Mechanism of Oxygen Activation,* Academic Press, New York, 1974.
5 (a) F. L. Urbah, in H. Siegel (ed.), *Metal Ions in Biological Systems,* Vol. 13, Marcel Dekker, New York, 1984, p. 73; (b) R. R. Gagné, C. L. Spiro, T. J. Smith, C. A. Hamann, W. R. Thies and A. K. Shiemke, *J. Am. Chem. Soc., 103* (1981) 4073.
6 A. B. P. Lever, B. S. Ramaswamy and S. R. Pickens, *Inorg. Chim. Acta, 46* (1980) L59.
7 O. Kahn, *Angew. Chem., Int. Ed. Engl., 24* (1985) 834.
8 (a) L. Banci, A. Bencini, D. Gatteschi and A. Dei, *Inorg. Chim. Acta, 36* (1979) L419; (b) L. Banci, A. Bencini, C. Benelli and D. Gatteschi, *Inorg. Chem., 21* (1982) 3868.
9 A. Bencini, D. Gatteschi and C. Zanchini, *Inorg. Chem., 24* (1985) 700.
10 A. Bencini, D.Gatteschi and C. Zanchini, *Inorg. Chem., 24* (1985) 704.
11 M. Boillot, Y. Journaux, A. Bencini, D. Gatteschi and O. Kahn, *Inorg. Chem., 24* (1985) 263.
12 W. J. Stratton and D. M. Busch, *J. Am. Chem. Soc., 82* (1960) 4834.
13 W. J. Stratton and P. J. Ogren, *Inorg. Chem., 9* (1970) 2588.
14 W. J. Stratton, *Inorg. Chem., 9* (1970) 517.
15 P. W. Ball and A. B. Blake, *J. Chem. Soc. A,* (1969) 1915.
16 J. Powell and A. Kuskis, *Can. J. Chem., 57* (1979) 2986.
17 K. S. Chong, S. J. Rettig, A. Storr and J. Trotter, *Can. J. Chem., 57* (1979) 3090.
18 K. S. Chong, S. J. Rettig, A. Storr and J. Trotter, *Can. J. Chem., 57* (1979) 3099.
19 K. S. Chong, S. J. Rettig, A. Storr and J. Trotter, *Can. J. Chem., 57* (1979) 3119.
20 J. E. Andrew, P. W. Ball and A. B. Blake, *J. Chem. Soc., Chem. Commun.,* (1969) 143.
21 L. G. Kuzmina, N. G. Bokii, A. V. Arutynyan, L. V. Rybin and M. I. Rybinskaya, *J. Struct. Chem., 12* (1971) 801.
22 P. W. Ball and A. B. Blake, *J. Chem. Soc., Dalton Trans.,* (1974) 852.
23 G. Marongiu and E. C. Lingafelter, *Acta Crystallogr., Sect. B, 38* (1982) 620.
24 A. J. Schouten, G. Chall and J. Reedijk, *J. Mol. Catal., 9* (1980) 41.
25 M. Ghedini, G. De Munno, G. Denti, A. M. Manotti Lanfredi and A. Tiripicchio, *Inorg. Chim. Acta, 57* (1982) 87.
26 M. Ghedini, F. Neve, F. Morazzoni and C. Oliva, *Polyhedron, 4*(3) (1985) 497.
27 J. E. Andrew and A. B. Blake, *J. Chem. Soc. A,* (1969) 1408.
28 L. K. Thompson, V. T. Chacko, J. A. Elvidge, A. B. P. Lever and R. V. Parish, *Can. J. Chem., 47* (1969) 4141.
29 W. Rosen, *Inorg. Chem., 10* (1971) 1832.
30 A. B. P. Lever, L. K. Thompson and W. M. Reiff, *Inorg. Chem., 11* (1972) 104.
31 A. B. P. Lever, L. K. Thompson and W. M. Reiff, *Inorg. Chem., 11* (1972) 2292.
32 D. A. Sullivan and G. J. Palenik, *Inorg. Chem., 16* (1977) 1127.
33 J. A. Doul and L. K. Thompson, *Can. J. Chem., 58* (1980) 221.
34 J. C. Dewan and L. K. Thompson, *Can. J. Chem., 60* (1982) 121.
35 D. V. Bautista, J. C. Dewan and L. K. Thompson, *Can. J. Chem., 60* (1982) 2583.
36 G. Bullock, F. W. Hartstock and L. K. Thompson, *Can. J. Chem., 61* (1983) 57.
37 L. K. Thompson, *Can. J. Chem., 61* (1983) 579.
38 P. Robichaud and L. K. Thompson, *Inorg. Chim. Acta, 85* (1984) 137.
39 D. Attanasio, G. Dessy and V. Fares, *Inorg. Chim. Acta, 104* (1985) 99.
40 L. K. Thompson, F. W. Harstock, L. Rosenberg and T. C. Woon, *Inorg. Chim. Acta, 97* (1985) 1; G. Paolucci, S. Cacchi and L. Caglioti, *J. Chem. Soc., Perkin Trans. 1,* (1979) 1129.
41 A. C. T. North, D. C. Philips, F. Matheus, *Acta Crystallogr., Sect. A, 24* (1968) 351.
42 *International Tables for X-ray Crystallgraphy,* Vol. 4, Kynoch, Birmingham, UK, 2nd edn., 1974, p. 101.
43 G. M. Sheldrick, *SHELX 76,* University of Cambridge, UK, 1976.
44 W. D. S. Motherwell and W. Clegg, *PLUTO,* Program for plotting molecular and crystal structures, University of Cambridge, UK, 1978.
45 C. J. O'Connor, E. Sinn, E. J. Cukauskas and B. S. Deaver, Jr., *Inorg. Chim. Acta, 32* (1979) 29.
46 C. J. O'Connor, in S. J. Lipard (ed), *Progress in Inorganic Chemistry,* Vol. 29, Wiley, New York, 1982, p. 208.
47 (a) G. Paolucci, G. Marangoni, G. Bandoli and D. A. Clemente, *J. Chem. Soc., Dalton Trans.,* (1980) 959; (b) (1980) 1404.

48 G. Paolucci, W. Cecchetti, R. Polloni, G. Frison and P. Traldi, *Inorg. Chim. Acta, 148* (1988) 151.

49 F. A. Cotton and G. Wilkinson, *Advanced Inorganic Chemistry,* Wiley, New York, 1980.

50 N. N. Greenwood and A. Earnshaw, *Chemistry of the Elements,* Pergamon, Oxford, 1985, p. 1345.

51 D. Webster and G. J. Palenik, *J. Chem. Soc., Chem. Commun.,* 74 (1975); *Inorg. Chem., 15* (1976) 755.

52 M. G. B. Drew, A. Lavery, V. McKee and S. M. Nelson, *J. Chem. Soc., Dalton Trans.,* (1985) 1771.

53 O. Kahn, I. Morgestern-Badarau, J. P. Audiere, J. M. Lehn and S. A. Sullivan, *J. Am. Chem. Soc., 102* (1980) 5935, and refs. therein; A. Earnshaw, *Introduction to Magnetochemistry,* Academic Press, New York, 1968, pp. 76–77.

54 P. W. Ball and B. Blake, *J. Chem. Soc. A,* (1969) 1415.

55 R. L. Lintvedt, L. L. Borer, D. P. Murtha, J. M. Kuszaji and M. D. Glick, *Inorg. Chem., 13* (1974) 18.

56 G. Paolucci, S. Stelluto, F. Benetollo and G. Bombieri, manuscript in preparation.

57 J. F. Geldard and F. Lions, *Inorg. Chem., 2* (1962) 2262; *J. Am. Chem. Soc., 84* (1962) 2262; R. W. Green, P. S. Hallmann and F. Lions, *Inorg. Chem., 3* (1964) 376.

58 G. Paolucci, S. Stelluto and R. Stevanato, *Abstr., XVIIIth National Conf. Inorganic Chemistry, Como, Italy, 1985,* A 14, 84.

59 G. Paolucci, V. Fratini, N. Stevanato and S. Stelluto, *Abstr., XXVth I.C.C.C., Nanjing, China, 1987,* C3, 626.